

# Active RIS-Aided Massive MIMO Uplink Systems with Low-Resolution ADCs

Zhangjie Peng, Zecheng Lu, Xue Liu, Cunhua Pan, *Senior Member, IEEE*, and Jiangzhou Wang, *Fellow, IEEE*

**Abstract**—This letter considers an active reconfigurable intelligent surface (RIS)-aided multi-user uplink massive multiple-input multiple-output (MIMO) system with low-resolution analog-to-digital converters (ADCs). The letter derives the closed-form approximate expression for the sum achievable rate (AR), where the maximum ratio combination (MRC) processing and low-resolution ADCs are applied at the base station. The system performance is analyzed, and a genetic algorithm (GA)-based method is proposed to optimize the RIS's phase shifts for enhancing the system performance. Numerical results verify the accuracy of the derivations, and demonstrate that the active RIS has an evident performance gain over the passive RIS.

**Index Terms**—Reconfigurable intelligent surface (RIS), active RIS, uplink achievable rate, massive MIMO, low-resolution ADCs.

## I. INTRODUCTION

Thanks to the capability of reconfiguring the radio propagation environment, reconfigurable intelligent surface (RIS) consisting of numerous reflecting elements has been considered as a breakthrough technology of 6th generation mobile networks [1], [2]. Specifically, RIS has low deployment costs and energy consumption while improving the performance and coverage of communication systems [3].

However, most of the existing contributions considered passive RIS. In fact, passive RIS suffers from “multiplicative fading”, which leads to severe signal attenuation and limits the system performance [4]. To solve this problem, active RIS equipped with active reflection-type amplifiers was proposed and regarded as a promising solution. This technology not only enables the adjustment of phase shifts but also amplifies the received signal at the cost of additional hardware power consumption [5], [6]. Recent contribution indicates that active RIS has a notable improvement over passive RIS under the same total network power consumption including both the transmit power and the hardware power consumption [7]. The researchers have explored the application of active RIS in various scenarios, such as multi-pair device-to-device (D2D) communications systems [8], mobile edge computing systems [9] and multiuser communication systems with hardware impairments [10].

Z. Peng, Z. Lu and X. Liu are with the College of Information, Mechanical and Electrical Engineering, Shanghai Normal University, Shanghai 200234, China. (e-mail: pengzhangjie@shnu.edu.cn; 1000511822@smail.shnu.edu.cn; 1000494962@smail.shnu.edu.cn).

C. Pan is with the National Mobile Communications Research Laboratory, Southeast University, Nanjing 210096, China. (e-mail: cpan@seu.edu.cn).

J. Wang is with the School of Engineering, University of Kent, CT2 7NT Canterbury, U.K. (e-mail: j.z.wang@kent.ac.uk).

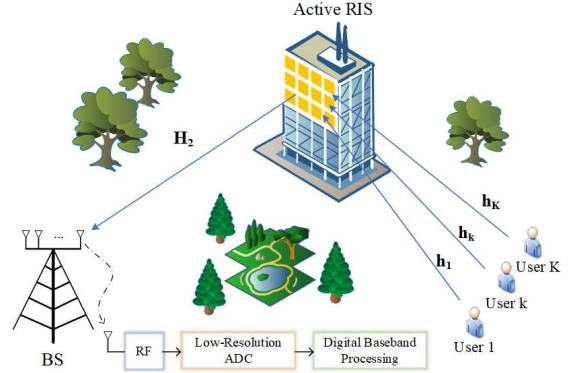


Fig. 1. Active RIS-aided massive MIMO uplink system with low-resolution ADCs.

Recently, researches have integrated RIS into massive multiple-input multiple-output (MIMO) communication systems, since it can greatly improve system performance [11]. With high-resolution digital-to-analog converters (DACs) or analog-to-digital converters (ADCs) equipped on each antenna, massive MIMO systems require substantial power consumption and cost expenditures. A promising solution for tackling this issues is to apply low-resolution ADCs/DACs in the systems because of its cost effectiveness [12]. The authors of [13] and [14] investigated low-resolution ADCs/DACs in passive RIS-aided massive MIMO systems and analyzed the system capacity.

However, as far as we are aware, the active RIS-aided multi-user uplink massive MIMO system with low-resolution ADCs has not been studied. The specific contributions of this letter are summarized as: 1) For an active RIS-aided multi-user uplink massive MIMO system with low-resolution ADCs, the closed-form approximate expression of the sum achievable rate (AR) is derived; 2) A genetic algorithm (GA)-based method is proposed to maximize the sum AR through the RIS's phase shifts optimization; 3) Extensive numerical results verify the accuracy of the derivations, and show the performance advantage of the active RIS and the rationality of applying low-resolution ADCs.

## II. SYSTEM MODEL

An active RIS-aided multi-user uplink massive MIMO system with low-resolution ADCs is depicted in Fig. 1. The direct communication links of this system are hindered owing to the obstacles. Hence, an active RIS with  $N$  reflecting elements is used to assist the communications between  $K$  single-antenna users and a base station (BS) that is composed of  $M$  antennas.

### A. Channel Model

All channels of this system follow the Rician fading. The users-RIS channel matrix  $\mathbf{H}_1 \in \mathbb{C}^{N \times K}$ , the  $k$ -th user-RIS channel vector  $\mathbf{h}_k \in \mathbb{C}^{N \times 1}$  for  $k \in \mathcal{S} \triangleq \{1, 2, \dots, K\}$  and the RIS-BS channel matrix  $\mathbf{H}_2 \in \mathbb{C}^{M \times N}$  are respectively expressed as

$$\mathbf{H}_1 = [\mathbf{h}_1, \dots, \mathbf{h}_k, \dots, \mathbf{h}_K], \quad (1)$$

$$\mathbf{h}_k = \sqrt{\alpha_k} \left( \sqrt{\frac{\varepsilon_k}{\varepsilon_k + 1}} \bar{\mathbf{h}}_k + \sqrt{\frac{1}{\varepsilon_k + 1}} \tilde{\mathbf{h}}_k \right), \quad (2)$$

$$\mathbf{H}_2 = \sqrt{\beta} \left( \sqrt{\frac{\delta}{\delta + 1}} \bar{\mathbf{H}}_2 + \sqrt{\frac{1}{\delta + 1}} \tilde{\mathbf{H}}_2 \right), \quad (3)$$

where  $\alpha_k$  and  $\beta$  stand for the corresponding large-scale fading coefficients. Vector  $\bar{\mathbf{h}}_k$  and matrix  $\bar{\mathbf{H}}_2$  denote the light-of-sight (LoS) parts. The parts of non-line-of-sight (NLoS) are respectively denoted by vector  $\tilde{\mathbf{h}}_k$  and matrix  $\tilde{\mathbf{H}}_2$  with independently and identically distributed (i.i.d) elements following the distribution of  $\mathcal{CN}(0, 1)$ .  $\varepsilon_k$  and  $\delta$  represent the Rician factors of  $\mathbf{h}_k$  and  $\mathbf{H}_2$ , respectively.

Assuming that uniform square planar arrays are adopted at the BS and the RIS,  $\bar{\mathbf{h}}_k$  and  $\bar{\mathbf{H}}_2$  can be respectively given by

$$\bar{\mathbf{h}}_k = \mathbf{a}_N(\phi_{kr}^a, \phi_{kr}^e), \quad (4)$$

$$\bar{\mathbf{H}}_2 = \mathbf{a}_M(\psi_{Rk}^a, \psi_{Rk}^e) \mathbf{a}_N^H(\phi_t^a, \phi_t^e), \quad (5)$$

where  $\phi_{kr}^a$  and  $\phi_{kr}^e$  are the azimuth and elevation angles of arrival (AOA) from the  $k$ -th user to the active RIS, respectively. Then,  $\phi_t^a$  and  $\phi_t^e$  stand for the azimuth and elevation angles of departure (AOD) at the BS from the active RIS, respectively.  $\psi_{Rk}^a$  and  $\psi_{Rk}^e$  represent the corresponding azimuth and elevation AOA at the BS from the active RIS. By denoting  $\lambda$  as the wavelength, the  $L$  dimensional array response vector  $\mathbf{a}_L(\varphi^a, \varphi^e)$  is given by

$$\mathbf{a}_L(\varphi^a, \varphi^e) = \left[ 1, \dots, e^{j2\pi \frac{d}{\lambda} (x \sin \varphi^e \sin \varphi^a + y \cos \varphi^e)}, \dots, e^{j2\pi \frac{d}{\lambda} ((\sqrt{L}-1) \sin \varphi^e \sin \varphi^a + (\sqrt{L}-1) \cos \varphi^e)} \right]^T, \quad (6)$$

where  $x = \lfloor (l-1)/\sqrt{L} \rfloor$ ,  $y = (n-1) \bmod \sqrt{L}$  and  $d$  is the elements spacing.

### B. Signal Transmission Model

The amplified signal at the active RIS can be represented as

$$\mathbf{y}_R = \mathbf{A}\Phi\mathbf{H}_1\mathbf{P}\mathbf{x} + \mathbf{A}\Phi\mathbf{v}, \quad (7)$$

where  $\mathbf{A} \triangleq \text{diag}\{\eta_1, \dots, \eta_n, \dots, \eta_N\} \in \mathbb{R}^{N \times N}$  is the amplification factor matrix and each element in the matrix is larger than 1.  $\mathbf{P} \triangleq \text{diag}\{\sqrt{p_1}, \dots, \sqrt{p_k}, \dots, \sqrt{p_K}\} \in \mathbb{R}^{K \times K}$ , where  $p_k$  denotes the transmit power of the  $k$ -th user. The reflecting coefficient matrix of the active RIS is denoted by  $\Phi = \text{diag}\{e^{j\theta_1}, \dots, e^{j\theta_N}\} \in \mathbb{C}^{N \times N}$ , and  $\theta_n \in [0, 2\pi)$  stands for the phase shift of element  $n$ .  $\mathbf{x} \triangleq [x_1, x_2, \dots, x_K]^T$  is the transmit symbol with  $\mathbb{E}\{|x_k|^2\} = 1$ . Owing to the application of the active components, we express  $\mathbf{A}\Phi\mathbf{v}$  as the dynamic noise [15], where  $\mathbf{v} \sim \mathcal{CN}(0_N, \sigma_v^2 \mathbf{I}_N)$ .

TABLE I  
 $\rho$  FOR DIFFERENT ADC QUANTIZATION BITS  $b$

$b$	1	2	3	4	5	$\geq 6$
$\rho$	0.3634	0.1175	0.03454	0.009479	0.002499	$\frac{\pi\sqrt{3}}{2} \cdot 2^{-2b}$

We assume that the values of each element in matrix  $\mathbf{A}$  are equal, i.e.,  $\eta_n \triangleq \eta$ . Thus, the reflecting signal power of the active RIS  $P_A \triangleq \mathbb{E}\{\|\mathbf{y}_R\|^2\}$  is calculated as

$$\begin{aligned} \mathbb{E}\{\|\mathbf{y}_R\|^2\} &= \mathbb{E}\{\|\mathbf{A}\Phi\mathbf{H}_1\mathbf{P}\mathbf{x} + \mathbf{A}\Phi\mathbf{v}\|^2\} \\ &= \text{Tr}\left(\mathbb{E}\left\{\left(\mathbf{A}\Phi\mathbf{H}_1\mathbf{P}\mathbf{x} + \mathbf{A}\Phi\mathbf{v}\right)\left(\mathbf{A}\Phi\mathbf{H}_1\mathbf{P}\mathbf{x} + \mathbf{A}\Phi\mathbf{v}\right)^H\right\}\right) \\ &= \eta^2 \left( \text{Tr}\left(\mathbb{E}\left\{\Phi\mathbf{H}_1\mathbf{P}\mathbb{E}\{\mathbf{x}\mathbf{x}^H\}\mathbf{P}^H\mathbf{H}_1^H\Phi^H\right\}\right) + \text{Tr}\left(\mathbb{E}\left\{\Phi\mathbf{v}\mathbf{v}^H\Phi^H\right\}\right) \right) \\ &= \eta^2 \text{Tr}\left(\mathbb{E}\left\{\mathbf{H}_1^H\mathbf{H}_1\mathbf{P}\mathbf{P}^H\right\}\right) + \eta^2 \text{Tr}\left(\mathbb{E}\left\{\mathbf{v}\mathbf{v}^H\right\}\right) \\ &= \eta^2 N \left( \sum_{k=1}^K p_k \alpha_k + \sigma_v^2 \right). \end{aligned} \quad (8)$$

The signal received at the BS is

$$\mathbf{y} = \mathbf{H}_2\mathbf{y}_R + \mathbf{n} = \mathbf{G}\mathbf{P}\mathbf{x} + \mathbf{H}_2\mathbf{A}\Phi\mathbf{v} + \mathbf{n}, \quad (9)$$

where  $\mathbf{G} \triangleq \mathbf{H}_2\mathbf{A}\Phi\mathbf{H}_1 \in \mathbb{R}^{M \times K}$  denotes the cascaded channel of the communication links and  $\mathbf{n} \sim \mathcal{CN}(0, \sigma_n^2 \mathbf{I}_M)$  stands for the additive white Gaussian noise (AWGN).

For reducing the costs of the actual deployment, this letter applies low-resolution ADCs on the basis of the additive quantization noise model (AQN) at the BS, and the quantized signal is obtained as [12]

$$\mathbf{y}_q = \alpha\mathbf{y} + \mathbf{n}_q = \alpha\mathbf{G}\mathbf{P}\mathbf{x} + \alpha\mathbf{H}_2\mathbf{A}\Phi\mathbf{v} + \alpha\mathbf{n} + \mathbf{n}_q, \quad (10)$$

where  $\alpha = 1 - \rho$ . Furthermore,  $\rho$  represents the inverse of the signal-to-quantization-noise ratio. The corresponding relationship between  $\rho$  and quantization bit  $b$  is listed in Table I.  $\mathbf{n}_q$  represents the additive Gaussian quantization noise vector, and the covariance of  $\mathbf{n}_q$  is obtained as

$$\mathbf{R}_{\mathbf{n}_q\mathbf{n}_q} = \alpha(1 - \alpha) \text{diag}\left(\mathbf{G}\mathbf{P}\mathbf{G}^H + \sigma_n^2 \mathbf{I}_M\right). \quad (11)$$

According to (10), the signal processed by maximal-ratio-combining (MRC) is given by

$$\mathbf{r} = \mathbf{G}^H \mathbf{y}_q = \alpha \mathbf{G}^H \mathbf{G} \mathbf{P} \mathbf{x} + \alpha \mathbf{G}^H \mathbf{H}_2 \mathbf{A} \Phi \mathbf{v} + \alpha \mathbf{G}^H \mathbf{n} + \mathbf{G}^H \mathbf{n}_q. \quad (12)$$

Hence, the signal transmitted by the  $k$ -th user can be further written as

$$\begin{aligned} r_k &= \alpha \sqrt{p_k} \mathbf{g}_k^H \mathbf{g}_k x_k + \alpha \sum_{i=1, i \neq k}^K \sqrt{p_i} \mathbf{g}_k^H \mathbf{g}_i x_i \\ &\quad + \eta \alpha \mathbf{g}_k^H \mathbf{H}_2 \Phi \mathbf{v} + \alpha \mathbf{g}_k^H \mathbf{n} + \mathbf{g}_k^H \mathbf{n}_q, \end{aligned} \quad (13)$$

where  $\mathbf{g}_k \triangleq \mathbf{H}_2 \mathbf{A} \Phi \mathbf{h}_k = \eta \mathbf{H}_2 \Phi \mathbf{h}_k$ . Then, the sum AR can be expressed as

$$R = \sum_{k=1}^K R_k, \quad (14)$$

where  $R_k$  represents the uplink AR of the  $k$ -th user. We give the expression of  $R_k$  in (15) at the bottom of the next page.

### III. ANALYSIS OF ACHIEVABLE UPLINK RATE

In this section, the closed-form approximate expression of the uplink AR is derived. Based on the expression, we can analyze the impact of various parameters on system performance.

**Theorem 1.** *For an active RIS-aided massive MIMO system with low-resolution ADCs and MRC processing, the uplink AR of the  $k$ -th user can be approximated as*

$$R_k \approx \log_2 \left( 1 + \frac{p_k \Gamma_1}{\sum_{i=1, i \neq k}^K p_i \Gamma_2 + \eta^2 \sigma_v^2 \Gamma_3 + \sigma_n^2 \Gamma_4 + \frac{1-\alpha}{\alpha} \Gamma_5} \right), \quad (16)$$

where  $\Gamma_1$ ,  $\Gamma_2$ ,  $\Gamma_3$ ,  $\Gamma_4$  and  $\Gamma_5$  are respectively given by  $\mathbb{E}\{\|\mathbf{g}_k\|^4\}$ ,  $\mathbb{E}\{\|\mathbf{g}_k^H \mathbf{g}_i\|^2\}$ ,  $\mathbb{E}\{\|\mathbf{g}_k^H \mathbf{H}_2 \Phi\|^2\}$ ,  $\mathbb{E}\{\|\mathbf{g}_k\|^2\}$  and  $\mathbb{E}\{\mathbf{g}_k^H \text{diag}(p_k \mathbf{G} \mathbf{G}^H + \sigma_A^2 \mathbf{I}_M) \mathbf{g}_k\}$  at the bottom of this page.

*Proof:* See Appendix. ■

According to Theorem 1, it indicates that the uplink AR of this system is affected by the number of BS antennas, the number of RIS reflecting elements, the large-scale fading coefficients, the transmit power, the noise power, the dynamic noise power, the Rician factors, the quantization bit, the AOA, the AOD and the power of active RIS.

Moreover, the power consumption model of the considered system is

$$P_T = P_t + P_A + N(P_{\text{SW}} + P_{\text{DC}}), \quad (22)$$

where  $P_t = \sum_{i=1}^K p_i$ .  $P_{\text{SW}}$  and  $P_{\text{DC}}$  represent the direct current biasing power and the power consumed by the switch and control circuit at each reflecting element, respectively [5]. The active RIS should meet the startup condition  $P_T \geq N(P_{\text{SW}} + P_{\text{DC}})$ , otherwise  $R_k = 0$ .

**Corollary 1.** *When  $\eta^2 = 1$  and  $\sigma_v^2 = 0$  in (16), the uplink AR in the case with passive RIS can be approximated as*

$$R_p \approx \log_2 \left( 1 + \frac{p_k \Gamma_1}{\sum_{i=1, i \neq k}^K p_i \Gamma_2 + \sigma_n^2 \Gamma_4 + \frac{1-\alpha}{\alpha} \Gamma_5} \right). \quad (23)$$

$$R_k = \mathbb{E} \left\{ \log_2 \left( 1 + \frac{p_k \alpha^2 \|\mathbf{g}_k\|^4}{\alpha^2 \sum_{i=1, i \neq k}^K p_i \|\mathbf{g}_k^H \mathbf{g}_i\|^2 + \eta^2 \alpha^2 \sigma_v^2 \|\mathbf{g}_k^H \mathbf{H}_2 \Phi\|^2 + \alpha^2 \sigma_n^2 \|\mathbf{g}_k\|^2 + \alpha(1-\alpha) \mathbf{g}_k^H \text{diag}(p_k \mathbf{G} \mathbf{G}^H + \sigma_n^2 \mathbf{I}_M) \mathbf{g}_k} \right) \right\}. \quad (15)$$

$$\Gamma_1 = \eta^4 M u_k^2 \left\{ M \delta^2 \varepsilon_k^2 |f_k(\Phi)|^4 + 2\delta \varepsilon_k |f_k(\Phi)|^2 \times (2MN + MN \varepsilon_k + MN + 2M + N \varepsilon_k + N + 2) + MN^2 (2\delta^2 + \varepsilon_k^2 + 2\delta \varepsilon_k + 2\delta + 2\varepsilon_k + 1) + N^2 (\varepsilon_k^2 + 2\delta \varepsilon_k + 2\delta + 2\varepsilon_k + 1) + MN(2\delta + 2\varepsilon_k + 1) + N(2\delta + 2\varepsilon_k + 1) \right\}, \quad (17)$$

$$\Gamma_2 = \eta^4 M u_k^2 u_i^2 \left\{ M \delta^2 \varepsilon_k \varepsilon_i |f_k(\Phi)|^2 |f_i(\Phi)|^2 + \delta \varepsilon_k |f_k(\Phi)|^2 (\delta MN + N \varepsilon_i + N + 2M) + \delta \varepsilon_i |f_i(\Phi)|^2 (\delta MN + N \varepsilon_k + N + 2M) + N^2 (M \delta^2 + \delta(\varepsilon_k + \varepsilon_i + 2) + (\varepsilon_i + 1)(\varepsilon_k + 1)) + MN(2\delta + \varepsilon_k + \varepsilon_i + 1) + M \varepsilon_k \varepsilon_i |\bar{\mathbf{h}}_k^H \bar{\mathbf{h}}_i|^2 + 2M \delta \varepsilon_k \varepsilon_i \text{Re}\{f_k^H(\Phi) f_i(\Phi) \bar{\mathbf{h}}_k^H \bar{\mathbf{h}}_i\} \right\}, \quad (18)$$

$$\Gamma_3 = \frac{\eta^2 M^2 \beta u_k}{(\delta + 1)} (\delta \varepsilon_k (2 + \delta N) |f_k(\Phi)|^2 + 2N\delta + N^2 \delta^2 + N \varepsilon_k + N) + \eta^2 MN \beta u_k (\delta \varepsilon_k |f_k(\Phi)|^2 + N\delta + N \varepsilon_k + N), \quad (19)$$

$$\Gamma_4 = \eta^2 M u_k (\delta \varepsilon_k |f_k(\Phi)|^2 + \delta N + \varepsilon_k N + N), \quad (20)$$

$$\Gamma_5 = p_k \eta^4 M u_k^2 \left\{ (\delta \varepsilon_k |f_k(\Phi)|^2)^2 + 4\delta \varepsilon_k |f_k(\Phi)|^2 (N(\delta + \varepsilon_k + 1) + 2) + 2N^2 (\delta + \varepsilon_k + 1)^2 + 2N(2\delta + 2\varepsilon_k + 1) \right\} + \eta^2 \sigma_n^2 M u_k (\delta \varepsilon_k |f_k(\Phi)|^2 + N(\delta + \varepsilon_k + 1)) + p_k \eta^4 M \sum_{i=1, i \neq k}^K \left\{ u_k u_i (\delta \varepsilon_k |f_k(\Phi)|^2 + N(\delta + \varepsilon_k + 1)) (\delta \varepsilon_i |f_i(\Phi)|^2 + N(\delta + \varepsilon_i + 1)) + 2\delta u_k u_i (\varepsilon_k \varepsilon_i \text{Re}\{f_k^H(\Phi) f_i(\Phi) \bar{\mathbf{h}}_k^H \bar{\mathbf{h}}_i\} + \varepsilon_k |f_k(\Phi)|^2 + \varepsilon_i |f_i(\Phi)|^2 + N) \right\}, \quad (21)$$

where  $f_s(\Phi) \triangleq \mathbf{a}_N^H (\phi_t^s, \phi_t^s) \Phi \bar{\mathbf{h}}_s$  and  $u_s \triangleq \frac{\beta \alpha_s}{(\delta + 1)(\varepsilon_s + 1)}$ ,  $s \in \{k, i\}$ .

### Algorithm 1 GA-Based Method

**Input:** A population  $P_1$  with  $N_{\text{total}}$  individuals, the iteration number  $i = 1$ , the number of the termination iteration times is  $i_T$ , and the termination value is  $f_i$ .

**Output:** maximum fitness function values

- 1: **while**  $i < i_T$  or  $\bar{f}$  (average change of the fitness value)  $< f_i$  **do**
- 2: Calculate the fitness value  $\bar{f}$  according to (16);
- 3: Select  $N_b$  individuals with large fitness function values as elites;
- 4: Select  $N_p$  parents ( $N_p \cap N_b = \emptyset$ ) for crossover to generate  $N_c$  offspring;
- 5: Use the remaining individuals for mutation to generate  $N_d$  offspring;
- 6: Add  $N_b$ ,  $N_c$  and  $N_d$  to the next population  $P_{i+1}$ ;  $i = i + 1$ .

The total power consumption is  $P_T = P_t' + N P_{\text{SW}}$  and the threshold condition is  $P_T \geq N P_{\text{SW}}$ .

**Corollary 2.** *With ideal ADCs ( $b \rightarrow \infty$ ,  $\alpha \rightarrow 1$ ), the uplink AR in (16) converges to  $R_k \rightarrow R_{\text{ideal}}$ , where*

$$R_{\text{ideal}} = \log_2 \left( 1 + \frac{p_k \Gamma_1}{\sum_{i=1, i \neq k}^K p_i \Gamma_2 + \eta^2 \sigma_v^2 \Gamma_3 + \sigma_n^2 \Gamma_4} \right), \quad (24)$$

which means the system has infinite precision. Due to  $b \rightarrow \infty$ , we consider that it is reasonable to ignore the quantization error of ADCs.

### IV. PHASE SHIFTS OPTIMIZATION

In this section, a GA-based method for optimizing phase shifts is proposed to enhance the system performance. The optimization problem is formulated as

$$\max_{\Phi} \sum_{k=1}^K R_k \quad (25)$$

$$\text{s.t. } \theta_n \in [0, 2\pi), \forall n, \quad (26)$$

where  $R_k$  is given by (16) in Theorem 1. The specific content of the GA-based method is displayed in Algorithm 1 at the top of this page.

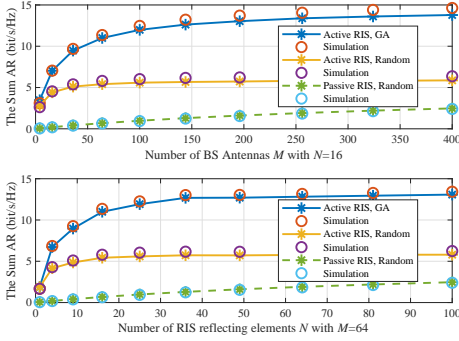


Fig. 2. The sum AR versus the number of BS antennas  $M$  and RIS reflecting elements  $N$  with  $b = 1$ .

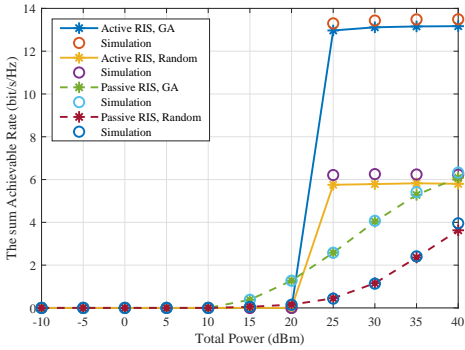


Fig. 3. The sum AR versus the total power  $P_T$  with  $b = 1$ .

## V. NUMERICAL RESULTS

In this part, we analyze the impacts of the number of BS antennas, the number of RIS elements, transmit power and quantization bits on the sum AR according to simulation results. Assuming the BS and the active RIS are respectively deployed at  $(0, 0, 25)$  and  $(5, 100, 30)$  in the simulation. In a semicircle centered at  $(5, 100, 1.6)$  with a radius of 5 metres, the users are randomly generated. We generate the AoA and AoD from  $[0, 2\pi]$  uniformly. For the consistency of the simulation, the generated angles will be fixed. We set other simulation values as follows: the number of users of  $K = 4$ , the number of BS antennas of  $M = 64$ , and the number of active RIS reflecting elements of  $N = 16$ . Noise power is  $\sigma_n^2 = -90$  dBm, dynamic noise is  $\sigma_v^2 = -70$  dBm [6], and Rician factors are  $\varepsilon_k = 10$ ,  $\delta = 1$ .  $P_T = 30$  dBm,  $P_{SW} = -10$  dBm and  $P_{DC} = -5$  dBm. The large-scale fading coefficient is expressed as  $Pathloss = -30 - 10\mathcal{T} \log_{10}(l)$ , where  $l$  denotes the distance of the  $k$ -th user to the RIS (or the RIS to the BS).  $\mathcal{T}$  is the path-loss exponent with  $\mathcal{T}_u = 2.8$  for the link of the  $k$ -th user to the RIS and  $\mathcal{T}_r = 2.8$  for the link of the RIS to the BS. To mitigate the spatial correlation between antennas,  $d$  is assumed to be  $\lambda/2$ . In addition, we eliminate the influence of randomness by averaging  $2 \times 10^4$  Monte Carlo realizations.

In Fig. 2, numerical results verify the correctness of the expression in Theorem 1 and Corollary 1, since the ‘‘Active RIS’’ and ‘‘Passive RIS’’ curves match well with the corresponding ‘‘Simulation’’ ones. We can find that the sum AR increases as  $M$  and  $N$  go larger, which provides guiding significance for deploying the RIS in the massive MIMO system. It is also obvious that compared to ‘‘Passive RIS’’, ‘‘Active RIS’’ is capable of approaching the upper limit of system performance

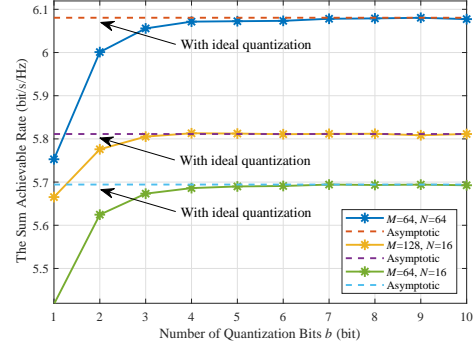


Fig. 4. The sum AR versus the number of quantization bits with different  $M$  and  $N$ .

while requiring fewer components such as  $M = 64$  and  $N = 16$ . In addition, the system performance can be notably enhanced by the method in Section IV.

Based on Fig. 3, we illustrate the impacts of the total power on the sum AR ( $N = 128$ ). It is obvious that when  $P_T$  is lower than 20 dBm, the sum AR of ‘‘Passive RIS’’ outperforms ‘‘Active RIS’’. Because the active RIS system consumes additional power  $P_{SW}$ , it has a higher startup threshold. However, ‘‘Active RIS’’ is able to achieve a higher rate under sufficient energy conditions. It means that active RIS can greatly alleviate ‘‘multiplicative fading’’ effect.

Fig. 4 depicts the sum AR under the quantization bit  $b$  of ADCs. Apparently, in cases with different  $M$  and  $N$ , the sum ARs initially increase fast with  $b$  and then gradually converge to different constants. More importantly, when  $b$  equals 4 bits, the system can achieve the similar performance to the case with high resolution ADCs. This means that the communication system in this letter can apply low-resolution ADCs to balance the system performance with the power consumption and hardware cost.

## VI. CONCLUSION

This letter studied an active RIS-aided massive MIMO system with low-resolution ADCs. We derived the closed-form approximate expression of the sum AR and applied a GA-based method to enhance the system performance. According to the numerical results, we validated the ultimate approximate expression and the algorithm’s efficacy. It also revealed that the active RIS has more performance advantages and applying low-resolution ADCs in this system can balance the system performance with the deployment costs.

## APPENDIX

The approximation of (16) has been readily proved in [16]. By using [11, Theorem 1],  $\mathbb{E}\{\|\mathbf{g}_k\|^4\}$ ,  $\mathbb{E}\{\|\mathbf{g}_k^H \mathbf{g}_i\|^2\}$  and  $\mathbb{E}\{\|\mathbf{g}_k\|^2\}$  can be easily obtained. Therefore, the main work that follows is to proof (19) and (21).

Firstly, we give the derivation of  $\mathbb{E}\{\|\mathbf{g}_k^H \mathbf{H}_2 \Phi\|^2\}$  as

$$\mathbb{E}\{\|\mathbf{g}_k^H \mathbf{H}_2 \Phi\|^2\} = \eta^2 \mathbb{E}\{\mathbf{h}_k^H \Phi^H \mathbf{H}_2^H \mathbf{H}_2 \mathbf{H}_2 \mathbf{H}_2 \Phi \mathbf{h}_k\}. \quad (27)$$

Then, we define  $\mathbf{W} \triangleq \mathbf{H}_2^H \mathbf{H}_2$ . The matrix  $\mathbf{W}$  satisfies non-central Wishart distribution  $\mathbf{W} \sim \mathcal{W}_N(M, \mathbf{S}, \Sigma)$ , where  $M$  is the degree of freedom,  $\mathbf{S} = \sqrt{\frac{\beta\delta}{1+\delta}} \bar{\mathbf{H}}_2$  is the mean

$$\begin{aligned}
\mathbb{E}\left\{|g_{km}|^2 |g_{im}|^2\right\} &= \eta^4 u_k u_i \mathbb{E}\left\{\sum_{c=1}^4 |g_{km}^c|^2 \sum_{c=1}^4 |g_{im}^c|^2\right\} + 4\eta^4 u_k u_i \left(\mathbb{E}\left\{\operatorname{Re}\left\{g_{km}^1 (g_{km}^3)^*\right\}\right\} \operatorname{Re}\left\{g_{im}^1 (g_{im}^3)^*\right\}\right) \\
&\quad + \mathbb{E}\left\{\operatorname{Re}\left\{g_{km}^1 (g_{km}^3)^*\right\}\right\} \operatorname{Re}\left\{g_{im}^2 (g_{im}^4)^*\right\}\right\} + \mathbb{E}\left\{\operatorname{Re}\left\{g_{km}^2 (g_{km}^4)^*\right\}\right\} \operatorname{Re}\left\{g_{im}^1 (g_{im}^3)^*\right\}\right\} + \mathbb{E}\left\{\operatorname{Re}\left\{g_{km}^2 (g_{km}^4)^*\right\}\right\} \operatorname{Re}\left\{g_{im}^2 (g_{im}^4)^*\right\}\right\} \\
&= \eta^4 u_k u_i \left(\delta \varepsilon_k |f_k(\Phi)|^2 + \delta N + \varepsilon_k N + N\right) \left(\delta \varepsilon_i |f_i(\Phi)|^2 + \delta N + \varepsilon_i N + N\right) \\
&\quad + 2\eta^4 u_k u_i \left(\varepsilon_k \varepsilon_i \operatorname{Re}\left\{f_k^H(\Phi) f_i(\Phi) \bar{\mathbf{h}}_k^H \bar{\mathbf{h}}_i\right\} + \varepsilon_k |f_k(\Phi)|^2 + \varepsilon_i |f_i(\Phi)|^2 + N\right), \tag{33}
\end{aligned}$$

$$\mathbb{E}\left\{|g_{km}|^4\right\} = \eta^4 u_k^2 \left\{\left(\delta \varepsilon_k |f_k(\Phi)|^2\right)^2 + 4\delta \varepsilon_k |f_k(\Phi)|^2 (N(\delta + \varepsilon_k + 1) + 2) + 2N^2 (\delta + \varepsilon_k + 1) + 2N(2\delta + 2\varepsilon_k + 1)\right\}, \tag{34}$$

where  $\mathbf{g}_k = \eta \mathbf{H}_2 \Phi \mathbf{h}_k = \eta u_k (\sqrt{\delta \varepsilon_k} \bar{\mathbf{H}}_2 \Phi \bar{\mathbf{h}}_k + \sqrt{\delta} \bar{\mathbf{H}}_2 \Phi \bar{\mathbf{h}}_k + \sqrt{\varepsilon_k} \bar{\mathbf{H}}_2 \Phi \bar{\mathbf{h}}_k + \bar{\mathbf{H}}_2 \Phi \bar{\mathbf{h}}_k)$ ,  $g_{km}$  is the  $m$ -th entry of  $\mathbf{g}_k$ .

matrix and  $\Sigma = \frac{\beta}{1+\delta} \mathbf{I}_N$  represents the covariance matrix. By approximation, the non-central Wishart matrix can be transformed into a central Wishart matrix [17]. In addition, the degree of freedom keeps the initial value while the covariance matrix can be  $\bar{\Sigma} = \Sigma + \frac{1}{M} \mathbf{S} \mathbf{S}^H = \frac{\beta}{1+\delta} (\mathbf{I}_N + \frac{\delta}{M} \bar{\mathbf{H}}_2^H \bar{\mathbf{H}}_2)$ , i.e.  $\mathbf{W} \sim \mathcal{W}_N(M, 0, \bar{\Sigma})$ . By applying the results in [18, Eq.(20)] and  $\operatorname{Tr}(\bar{\Sigma}) = N\beta$ , we have

$$\begin{aligned}
\mathbb{E}\left\{\mathbf{H}_2^H \mathbf{H}_2 \mathbf{H}_2^H \mathbf{H}_2\right\} &= \mathbb{E}\left\{\mathbf{W} \mathbf{W}\right\} = M \bar{\Sigma} (M \bar{\Sigma} + \operatorname{Tr}(\bar{\Sigma})) \\
&= \frac{M^2 \beta^2}{(\delta + 1)^2} (\mathbf{I}_N + \frac{2\delta}{M} \bar{\mathbf{H}}_2^H \bar{\mathbf{H}}_2 + \frac{\delta^2}{M^2} \bar{\mathbf{H}}_2^H \bar{\mathbf{H}}_2 \bar{\mathbf{H}}_2^H \bar{\mathbf{H}}_2) \\
&\quad + \frac{MN\beta^2}{(\delta + 1)^2} (\mathbf{I}_N + \frac{\delta}{M} \bar{\mathbf{H}}_2^H \bar{\mathbf{H}}_2). \tag{28}
\end{aligned}$$

Thus, (27) can be reformulated as

$$\begin{aligned}
\mathbb{E}\left\{\mathbf{h}_k^H \Phi^H \mathbf{H}_2^H \mathbf{H}_2 \mathbf{H}_2^H \mathbf{H}_2 \Phi \mathbf{h}_k\right\} &= \mathbb{E}\left\{\frac{M^2 \beta^2}{(\delta + 1)^2} (\mathbf{h}_k^H \mathbf{h}_k \right. \\
&\quad \left. + \frac{2\delta}{M} \mathbf{h}_k^H \Phi^H \bar{\mathbf{H}}_2^H \bar{\mathbf{H}}_2 \Phi \mathbf{h}_k + \frac{\delta^2}{M^2} \mathbf{h}_k^H \Phi^H \bar{\mathbf{H}}_2^H \bar{\mathbf{H}}_2 \bar{\mathbf{H}}_2^H \bar{\mathbf{H}}_2 \Phi \mathbf{h}_k) \right. \\
&\quad \left. + \frac{MN\beta^2}{(\delta + 1)^2} (\mathbf{h}_k^H \mathbf{h}_k + \frac{\delta}{M} \mathbf{h}_k^H \Phi^H \bar{\mathbf{H}}_2^H \bar{\mathbf{H}}_2 \Phi \mathbf{h}_k)\right\}, \tag{29}
\end{aligned}$$

where  $\mathbb{E}\left\{\mathbf{h}_k^H \mathbf{h}_k\right\} = N\alpha_k$  and the other terms can be calculated as

$$\begin{aligned}
\mathbb{E}\left\{\mathbf{h}_k^H \Phi^H \bar{\mathbf{H}}_2^H \bar{\mathbf{H}}_2 \Phi \mathbf{h}_k\right\} &= \operatorname{Tr}(\mathbb{E}\left\{\mathbf{h}_k^H \Phi^H \bar{\mathbf{H}}_2^H \bar{\mathbf{H}}_2 \Phi \mathbf{h}_k\right\}) \\
&= \frac{M\alpha_k \varepsilon_k}{\varepsilon_k + 1} \mathbb{E}\left\{\|\mathbf{a}_N^H(\phi_t^a, \phi_t^e) \Phi \bar{\mathbf{h}}_k\|^2\right\} + \frac{MN\alpha_k}{\varepsilon_k + 1} \\
&= \frac{M\alpha_k}{\varepsilon_k + 1} (\varepsilon_k |f_k(\Phi)|^2 + N), \tag{30}
\end{aligned}$$

$$\mathbb{E}\left\{\mathbf{h}_k^H \Phi^H \bar{\mathbf{H}}_2^H \bar{\mathbf{H}}_2 \bar{\mathbf{H}}_2^H \bar{\mathbf{H}}_2 \Phi \mathbf{h}_k\right\} = \frac{M^2 N \alpha_k}{\varepsilon_k + 1} (\varepsilon_k |f_k(\Phi)|^2 + N). \tag{31}$$

Then, (19) can be obtained by substituting (29) into (27).

Secondly,  $\mathbb{E}\left\{\mathbf{g}_k^H \operatorname{diag}(p_k \mathbf{G} \mathbf{G}^H + \sigma_n^2 \mathbf{I}_M) \mathbf{g}_k\right\}$  can be expanded as

$$\begin{aligned}
&\mathbb{E}\left\{\mathbf{g}_k^H \operatorname{diag}(p_k \mathbf{G} \mathbf{G}^H + \sigma_n^2 \mathbf{I}_M) \mathbf{g}_k\right\} \\
&= \mathbb{E}\left\{\sum_{m=1}^M |g_{km}|^2 \left(p_k \sum_{i=1, i \neq k}^K |g_{im}|^2 + p_k |g_{km}|^2 + \sigma_n^2\right)\right\} \\
&= p_k \sum_{m=1}^M \sum_{i=1, i \neq k}^K \mathbb{E}\left\{|g_{km}|^2 |g_{im}|^2\right\} + p_k \sum_{m=1}^M \mathbb{E}\left\{|g_{km}|^4\right\} \\
&\quad + \sigma_n^2 \sum_{m=1}^M \mathbb{E}\left\{|g_{km}|^2\right\}, \tag{32}
\end{aligned}$$

where  $\mathbb{E}\left\{|g_{km}|^2\right\} = \frac{1}{M} \mathbb{E}\left\{\|\mathbf{g}_k\|^2\right\}$  is obtained by (20). In addition,  $\mathbb{E}\left\{|g_{km}|^2 |g_{im}|^2\right\}$  and  $\mathbb{E}\left\{|g_{km}|^4\right\}$  are respectively given in (33) and (34) at the beginning of this page. We can calculate (21) by substituting (20), (33) and (34) into (32). Hence, Theorem 1 is proved.

## REFERENCES

- [1] C. Pan, G. Zhou, K. Zhi, S. Hong, T. Wu, Y. Pan, H. Ren, M. D. Renzo, A. Lee Swindlehurst, R. Zhang, and A. Y. Zhang, "An overview of signal processing techniques for RIS/IRS-aided wireless systems," *IEEE J. Sel. Topics Signal Process.*, vol. 16, no. 5, pp. 883–917, Aug. 2022.
- [2] Z. Zhang and L. Dai, "A joint precoding framework for wideband reconfigurable intelligent surface-aided cell-free network," *IEEE Trans. Signal Process.*, vol. 69, pp. 4085–4101, Jun. 2021.
- [3] Q. Wu and R. Zhang, "Intelligent reflecting surface enhanced wireless network via joint active and passive beamforming," *IEEE Trans. Wireless Commun.*, vol. 18, no. 11, pp. 5394–5409, Nov. 2019.
- [4] E. Björnson, Ö. Özdogan, and E. G. Larsson, "Intelligent reflecting surface versus decode-and-forward: How large surfaces are needed to beat relaying?" *IEEE Trans. Wireless Lett.*, vol. 9, no. 2, pp. 244–248, Feb. 2020.
- [5] R. Long, Y.-C. Liang, Y. Pei, and E. G. Larsson, "Active reconfigurable intelligent surface-aided wireless communications," *IEEE Trans. Wireless Commun.*, vol. 20, no. 8, pp. 4962–4975, Aug. 2021.
- [6] C. You and R. Zhang, "Wireless communication aided by intelligent reflecting surface: Active or passive?" *IEEE Wireless Commun. Lett.*, vol. 10, no. 12, pp. 2659–2663, Dec. 2021.
- [7] K. Zhi, C. Pan, H. Ren, K. K. Chai, and M. El-kashlan, "Active RIS versus passive RIS: Which is superior with the same power budget?" *IEEE Commun. Lett.*, vol. 26, no. 5, pp. 1150–1154, May 2022.
- [8] Z. Peng, X. Liu, C. Pan, L. Li, and J. Wang, "Multi-pair D2D communications aided by an active RIS over spatially correlated channels with phase noise," *IEEE Wireless Commun. Lett.*, vol. 11, no. 10, pp. 2090–2094, Oct. 2022.
- [9] Z. Peng, R. Weng, Z. Zhang, C. Pan, and J. Wang, "Active reconfigurable intelligent surface for mobile edge computing," *IEEE Wireless Commun. Lett.*, vol. 11, no. 12, pp. 2482–2486, Dec. 2022.
- [10] Z. Peng, Z. Zhang, C. Pan, M. Di Renzo, O. A. Dobre, and J. Wang, "Beamforming optimization for active RIS-aided multiuser communications with hardware impairments," *IEEE Trans. Wireless Commun.*, Feb. 2024, early access, doi: 10.1109/TWC.2024.3367131.
- [11] K. Zhi, C. Pan, H. Ren, and K. Wang, "Power scaling law analysis and phase shift optimization of RIS-aided massive MIMO systems with statistical CSI," *IEEE Trans. Commun.*, vol. 70, no. 5, pp. 3558–3574, May 2022.
- [12] L. Fan, S. Jin, C.-K. Wen, and H. Zhang, "Uplink achievable rate for massive MIMO systems with low-resolution ADC," *IEEE Commun. Lett.*, vol. 19, no. 12, pp. 2186–2189, Oct. 2015.
- [13] Z. Peng, X. Chen, C. Pan, M. El-kashlan, and J. Wang, "Performance analysis and optimization for RIS-assisted multi-user massive MIMO systems with imperfect hardware," *IEEE Trans. Veh. Technol.*, vol. 71, no. 11, pp. 11786–11802, Nov. 2022.
- [14] J. Dai, Y. Wang, C. Pan, K. Zhi, H. Ren, and K. Wang, "Reconfigurable intelligent surface aided massive MIMO systems with low-resolution DACs," *IEEE Commun. Lett.*, vol. 25, no. 9, pp. 3124–3128, Sep. 2021.
- [15] Z. Zhang, L. Dai, X. Chen, C. Liu, F. Yang, R. Schober, and H. V. Poor, "Active RIS vs. passive RIS: Which will prevail in 6G?" *IEEE Trans. Commun.*, vol. 71, no. 3, pp. 1707–1725, Mar. 2023.
- [16] Q. Zhang, S. Jin, K. Wong, H. Zhu, and M. Matthaiou, "Power scaling of uplink massive MIMO systems with arbitrary-rank channel means," *IEEE J. Sel. Topics Signal Process.*, vol. 8, no. 5, pp. 966–981, Oct. 2014.
- [17] H. Steyn and J. Roux, "Approximations for the non-central wishart distribution," *South African Statist J.*, vol. 6, no. 2, pp. 165–173, 1972.
- [18] J. A. Tague and C. I. Caldwell, "Expectations of useful complex wishart forms," *Multidimensional Syst. & Signal Process.*, vol. 5, no. 3, pp. 263–279, 1994. [Online]. Available: <https://doi.org/10.1007/BF00980709>

This figure "active\_RIS.png" is available in "png" format from:

<http://arxiv.org/ps/2404.13875v1>